

Natural Convection on Pleural Fluid Flow with Applied Magnetic Field over Covid -19

Usha G

Department of Mathematics, VISTAS, Vels University

Chennai, India

ushagovind2014@gmail.com

Dr. S. Senthamil Selvi

Department of Mathematics, VISTAS, Vels University

Chennai, India

msselvi2305@gmail.com

Padmavathi Thiyagarajan

Department of Mathematics, VISTAS, Vels University

Chennai, India

0000-0001-6073-0468

Received: 2022 March 15; **Revised:** 2022 April 20; **Accepted:** 2022 May 10

Abstract— Massive droplet transmission is primarily responsible for the COVID-19 pandemic consequences, which are the most serious. Pleural effusion is a primary symptom of coronavirus illness. Direct contact with infected people can result in droplet transmission of the COVID-19 virus, as can indirectly contact nearby surfaces or things used on the infected person. The physics of the pleural fluid deformation in the lung on free convection is described in the current paper. A pleural effusion happens when fluid accumulates between the lung and the chest wall. With excess fluid, the lung's surrounding tissue could become irritated. There are numerous causes for this, including pneumonia. Graphical representations of the various velocity, temperature, and concentration profiles are produced by varying the non-dimensional parameters of the fluid.

Keywords— COVID-19, Direct Droplet transmission, Natural convection, Pleural effusion.

I. INTRODUCTION

The spread of diseases via droplets has long been a subject of intense research in many domains. Concerns about the spread of the infectious COVID-19 disease include the transmission of bacterial and viral infections from inanimate surfaces to vulnerable individuals. When an infected person breathes infectious organisms such as influenza, COVID-19, or SARS viruses, airborne disease transmission begins. Complex flow processes, such as air-mucous contact, turbulence and droplet evaporation, deposition, flow-induced particle dispersion, and sedimentation, moderate the transmission process. Droplets more significant than a specific size settle more quickly than they evaporate, contaminating nearby surfaces. Because they are smaller, drops evaporate more rapidly than they do.

The entire respiratory system is constantly exposed to air; most particles are removed by inhalation, but aspiration, mucosal dissemination, and homogenous spread all happen. Few bacterial or viral infections manifest as particular surface antigens adhering to mucosal epithelial cells in people with healthy lungs. An excessive fluid buildup between a human lung and the chest wall is a pleural effusion. Pleura surround each of our human lungs. A thin membrane known as the pleura lines the interior of the chest wall and covers the lungs. The two occupied pleura levels often have a small fluid between them. The lungs

and chest wall move when we breathe, which functions as lubricating oil between them.

Various treatments bring numerous pleural effusions that are brought on by multiple treatments. A low blood protein level increases blood vessel pressure, or fluid spills into the pleural space, which are the three leading causes of transudative pleural effusion. Heart failure is the most typical cause. Exudative effusion is brought on by tumors, infections, or obstructed blood arteries.

The patient noticed a differential diagnosis of dyspnea and dry cough referred to lung cancer and was treated for the COVID-19 infection, according to Zahra Ahmadinejad et al., [1]. Saffman [2], who was interested in the impacts of both coarse and fine dust, looked into the influence of the crucial Reynolds number on the change from laminar to turbulent flow. According to Adrian Bejan, the order-of-magnitude estimations generated by scale analysis were validated by the buoyancy ratio and Lewis number simultaneously multiple-scale boundary-layer problem [3]. Christian et al., [4] lung parenchyma computations assessed and identified as nonlinear compressible in various computational lung models. Experiments are compared with whole pulmonary to allow the model to be validated in vivo. Richard Haber [5] the correct fluid dynamic forces on the lung that balance buoyancy and allow for stable states of the pleura not coming into contact. Pleural fluid

pressure can simultaneously balance the buoyancy of the lung. The unstable free convective mass transfer flow past an infinite vertical plate with changing suction velocity was studied by Ramana Reddy [6] for both Soret and MHD effects. Mittal et al., [7] has attempted to demonstrate the flow mechanics of the COVID-19 epidemic, including the generation of respiratory droplets, two-phase expiratory fluxes, and droplet evaporation. S. Das and others [8] The radiative heat flux was modeled using the Rosseland diffusion approximation in the energy equation. The Laplace transform method has been used to reach conclusions regarding an infinite vertical plate with heat and mass transport in the presence of thermal radiation. Using a sliding semi-infinite shear scale and the influence of chemical reactions during mixed convection, Prakash [9] described a perturbation technique. The ongoing problem from a moving vertical surface by R. Muthucumaraswamy [10]. Using a specified physical norm, Swetaprovo Chaudhuri [11] theoretically developed respiratory droplet dynamics and pandemic droplet evaporation. The current study focuses on how the natural buoyancy effect of the lungs causes pleural fluid to get contaminated by a new coronavirus. Padmavathi et al., [12]-[15] established various respiratory tract fluid flow due to forced and free convection stream.

A. MATHEMATICAL FORMULATION

We have taken into account an unsteady two-dimensional laminar flow of a viscous, incompressible fluid (Pleural Fluid) of uniform cross section h , fluid is lying above and below bounded by porous layers, and the physical situation can be written in Cartesian form under the assumptions based on study areas. The initial time-dependent slip boundary condition at the porous medium interface at $t \leq 0$, assumes that the region is at the same temperature T and concentration C . When $t > 0$, the temperature and concentration of the area instantly rise to T_0 and C_0 , respectively. These values oscillate with time and are thus kept constant. Make the x axis parallel to the fluid flow and the y axis perpendicular. The problem's schematic representation is displayed below. The appropriate boundary conditions are used to derive the governing equation and the ensuing assumptions are then generated. In the y direction, the blood flow is subjected to a consistent magnetic field, designated B_0 . The mobility of COVID-19 barely creates any applied magnetic field or electric field. Over the model, the Boussinesq approximation is used.

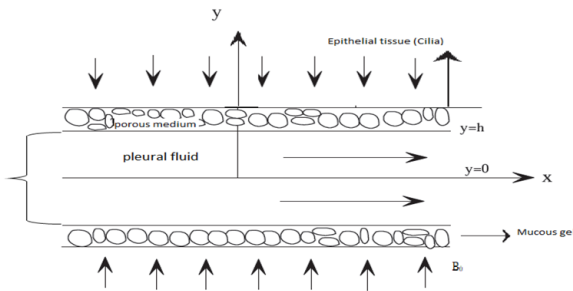


Fig:1 Physical Configuration

The balances of the mass, linear momentum, energy, and concentration species serve as the foundation for the governing equations.

Continuity Equation:

$$\frac{\partial u}{\partial x} + \frac{\partial v}{\partial y} = 0 \tag{1}$$

Navier-stokes Equation:

$$\frac{\partial u}{\partial t} + u \frac{\partial u}{\partial x} + v \frac{\partial u}{\partial y} = -\frac{1}{\rho} \frac{\partial p}{\partial x} + \nu \left(\frac{\partial^2 u}{\partial x^2} + \frac{\partial^2 u}{\partial y^2} \right) + g\beta(T - T_0) + g\beta^*(C - C_0) - \frac{\nu}{\sqrt{k_1}} u - \frac{u\sigma\beta_0}{\rho} \tag{2}$$

By substituting the following non-dimensional quantities, the given problem becomes non-dimensional.

$$u^* = \frac{u}{v_0}, v^* = \frac{v}{v_0}, x^* = \frac{xv_0}{\nu}, y^* = \frac{yv_0}{\nu}, \theta^* = \frac{T - T_0}{T_a - T_0}, \varphi^* = \frac{C - C_0}{C_a - C_0}, t^* = \frac{tv_0^2}{\nu}, p^* = \frac{p}{\rho v_0^2}$$

where temperature and concentration are represented by the dimensionless variables θ and φ respectively.

Neglecting the (*) symbol results in the main governing Equations (1) and (2) no longer implying $v = v_0$, where v_0 is a real positive constant and is also taken into account as the characteristic velocity.

$$\frac{\partial v}{\partial y} = 0 \tag{3}$$

$$\frac{\partial u}{\partial t} + v \frac{\partial u}{\partial y} = -\frac{\partial p}{\partial x} + \left(\frac{\partial^2 u}{\partial y^2} \right) + Gr\theta + Gc\varphi - \sigma^* u - H_a^* u \tag{4}$$

Using non-dimensional values, the beginning and boundary condition becomes,

$$\left. \begin{aligned} \text{At, } t = 0, \quad u = 0 \\ \text{At, } y = 0, \quad u = 0 \\ \text{At, } y = H, \quad \frac{\partial u}{\partial y} = \alpha\sigma u, \quad \frac{\partial \theta}{\partial y} = \alpha\sigma(\theta + T_{x3}) \end{aligned} \right\} \tag{5}$$

Where, $Gr = \frac{g\beta\nu(T_w - T_0)}{v_0^3}$ [Grashof number], $Gc = \frac{g\beta^*\nu(C_w - C_0)}{v_0^3}$ [Solutal Grashof number],

$$\sigma = \frac{\nu}{v_0\sqrt{k_1}}, [Porosity\ parameter] H_a = \frac{\nu\sigma\beta_0}{\rho v_0^2} [Hartmann\ number]$$

B. SOLUTION METHOD

The perturbation method can be used to obtain the analytical solution for the set of dimensionless equations from (3) - (4), along with the set of boundary conditions (5). This procedure can be carried out

by depicting the perturbation parameter ($\epsilon \ll 1$) as being very, very small and then following it with flow velocity u .

$$U(x, y, t) = u_0(y) + \epsilon e^{(\lambda t + \mu x)} u_1(y) + o(\epsilon^2) \quad (6)$$

$$P(x, y, t) = p_0(x) + \epsilon e^{(\lambda t + \mu x)} p_1(y) + o(\epsilon^2) \quad (7)$$

By substituting the aforementioned equation into the basic equations (6) to (7), we can move further with our problem while ignoring higher order terms, i.e., $o(\epsilon^2)$. The resulting set of equations are as follows

$$\left(\frac{\partial^2 u_0}{\partial y^2} \right) - C_t \frac{\partial u_0}{\partial y} - (\sigma^2 + H_a^2) u_0 = \frac{\partial p_0}{\partial x} - Gr \theta_0 - Gc \varphi_0 \quad \text{and} \quad u_1$$

$$\text{At } y = 0, \quad u_0 = 0, \quad (9)$$

$$\text{At } y = H, \quad \frac{\partial u_0}{\partial y} = \alpha \sigma u_0,$$

Boundary conditions (9) can be used to obtain zeroth-order velocity (u_0), We get,

$$u_0 = A_9 e^{m_9 y} + A_{10} e^{m_{10} y} - \frac{g_1}{N} - (R_1 e^{m_1 y} + R_2 e^{m_2 y} + C_1 e^{m_3 y} + C_2 e^{m_6 y}) \quad (10) \text{ At } y = 0, \quad u_1 = 0, \quad (11)$$

$$\text{At } y = H, \quad \frac{\partial u_1}{\partial y} = \alpha \sigma u_1$$

Boundary conditions (11) can be used to simultaneously derive first order velocity (u_1), We get,

$$u_1 = A_{11} e^{m_{11} y} + A_{12} e^{m_{12} y} - \frac{g_1}{N} - (R_3 e^{m_3 y} + R_4 e^{m_4 y} + C_3 e^{m_7 y} + C_4 e^{m_8 y}) \quad (12)$$

II RESULT AND DISCUSSIONZ

The goal of the current study is to assess how well numerical computations of the analytical results for the following fluid particles velocity distributions can characterize the flow of the fluid at various values of physical parameters. MATHEMATICA 12.0 was used to compute the heat and mass transport, and the findings are also displayed graphically. To evaluate the graph throughout the algorithm, we use equivalent values. Until the other parameter values are maintained in their fixed state. The Grashof number, Hartmann number, Porosity parameter are among the parameters we are computing.

$$(t = 2, \mu = 3 \times 10^{-6}, \rho = 992.2 \times 10^{-15}, g = 9.81 \times 10^6, C_t = 0.001, \lambda = 0.005, \epsilon = 0.002, n = 0.001, x = 0.01, H = 0.5, Gr = 0.5, Gc = 0.5, \alpha = 0.4, \sigma = 0.4, K = 0.5, M = 0.3, \sigma = 0.4, Q = 0.2, \epsilon = 0.03)$$

Fig. 2 depicts how different magnetic fields affect the velocity distribution. Lorentz force is the way of referring to such a force. The graph below shows that the fluid's velocity rises as the HARTMANN parameter increases. A solid material's porosity is a measure of the "Empty space," whose volume ranges from 0 to 1. We noticed that the fluid's velocity rises as the porosity permeable parameter rises. The pleural fluid's velocity is depicted in the aforementioned graphs as increasing pictorially as the values of the Grashof and Solutal Grashof parameters. It is evident that a buoyant flow develops during fluid flow inside the lung as a result of the gravitational force's acceleration move through fluids.

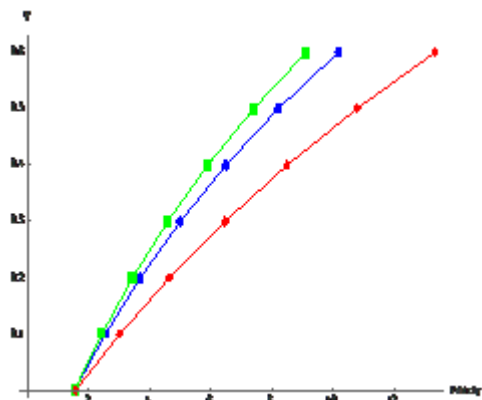


Fig. 2. Velocity field for various values of Ha

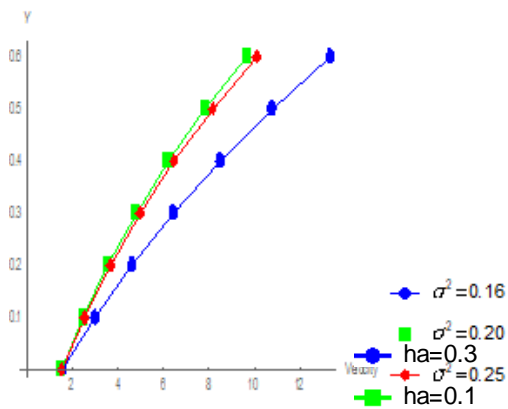


Fig. 3. Velocity field for various values of σ^*

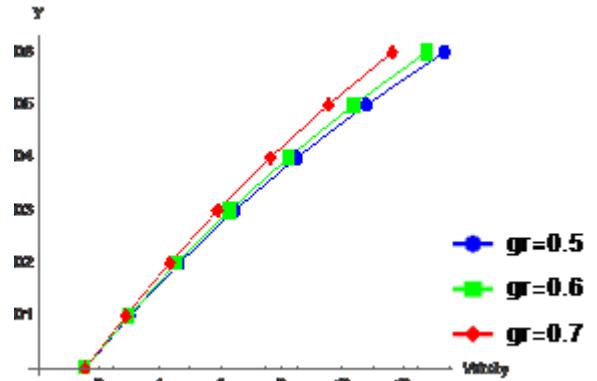


Fig. 4. Velocity field for various values of Gr

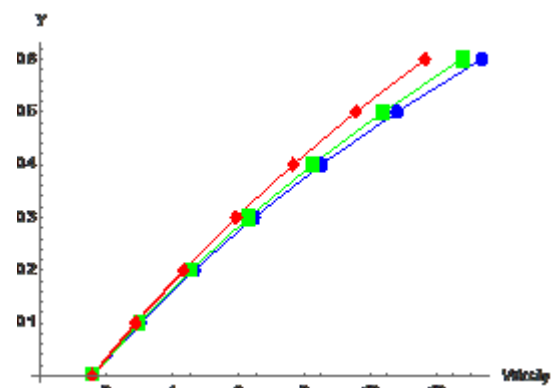


Fig. 5. Velocity field for various values of Gc

III CONCLUSIONS

In the use of the perturbation technique, the dimensionless governing equations above are analytically resolved. We have come to the conclusion that the buoyancy effect of the lungs and chemical reactions within the pleural cavity cause heat and mass to transfer on an unstable magnetic field with natural convection flow of the human respiratory system.

The key conclusions from the aforementioned results are as follows:

- As the Hartmann number and porosity parameter grow, the velocity of a fluid flow increases monotonically.

- Both the Grashof and Solutal Grashof number and the fluid flow velocity gradually rise.

IV Nomenclature

- $u, v \rightarrow$ the fluid flow velocity in x and y direction.
 $g \rightarrow$ gravitational acceleration
 $p \rightarrow$ pressure of the fluid
 $\rho \rightarrow$ fluid density
 $\mu \rightarrow$ dynamic viscosity of the pleural fluid
 $\nu \rightarrow$ kinematic viscosity of the pleural fluid
 $Gr \rightarrow$ Grashof Number
 $Gc \rightarrow$ Solutal Grashof Number
 $Ha \rightarrow$ Hartmann Number
 $\sigma^* \rightarrow$ Porosity Parameter

REFERENCES

- [1] Zahra Ahmadinejad, Faeze Salah hour, Omid Dadras, Hesam Rezaei, Syeed Ahmad Alinaghi* "Pleural Effusion as a Sign of Coronavirus Disease 2019 (COVID-19) Pneumonia: A Case Report". *Journal of Infectious Disorders - Drug Targets* DOI : 10.2174/1871526520666200609125045
- [2] Saffman.P.G., (1962). On the stability of laminar flow of a dusty gas. *J.Fluid Mech*, 13, 120-134.
- [3] Adrian Bejan, R. and Khair, Heat and mass transfer by natural convection in a porous medium, *Int. J.Heat Mass Transfer*, 28 (1985) 909-918.
- [4] Christian J. Roth, Lena Yoshihara, Mahmoud Ismail, Wolfgang A. Wall*, Computational modelling of the respiratory system: Discussion of coupled modelling approaches and two recent extensions, *Journal of Comput. Methods Appl. Mech. Engg.* 314 (2017) 473–493.
- [5] Richard Haber James B. Grotberg, Matthew R. Glucksberg ,Giuseppe Misericchi Daniele Venturoli, Massimo Del Fabbro, Christopher M. Waters, Steady-State Pleural Fluid Flow and Pressure and the Effects of Lung Buoyancy , *J. of Biomechanical Engineering* OCTOBER (2001)Vol. 123, 485- 492.
- [6] G. V. Ramana Reddy1, Ch. V. Ramana Murthy2, and N. Bhaskar Reddy3, Unsteady Mhd Free Convective Mass Transfer Flow Past An Infinite Vertical Porous Plate With Variable Suction And Soret Effect, *Int. J. of Appl. Math and Mech.* 7 (21): 70-84, 2011.
- [7] R. Mittal, R. Ni and J.-H. Seo, The flow physics of COVID-19, *J. Fluid Mech.* (2020), vol. 894, F2.
- [8] S. Das1, R. N. Jana2 and A. J. Chamkha3, Unsteady Free Convection Flow past a Vertical Plate with Heat and Mass Fluxes in the Presence of Thermal Radiation, *Journal of Applied Fluid Mechanics*, Vol. 8, No. 4, pp. 845-854, 2015.
- [9] J. Prakash1, R. Sivaraj2 & B. Rushi Kumar2, Influence of chemical reaction on unsteady MHD mixed convective flow over

- a moving vertical porous plate, *International Journal of Fluid Mechanics* 3(1) (2011) 1-14.
- [10] R.Muthucumaraswamy, Effects of a chemical reaction on a moving isothermal vertical surface with suction, *Acta Mechanica*,155, March -(2002) 65-70.
- [11] Swetaprovo Chaudhuri^{1,a}), Saptarshi Basu^{2,b}), Prasenjit Kabi², Vishnu R. Unni³, and Abhishek Saha^{3,c}) , Modelling the role of respiratory droplets in Covid-19 type pandemics. *Journal Physics of Fluids* 32, 063309 (2020); <https://doi.org/10.1063/5.0015984>
- [12] Padmavathi Thiyagarajan, Sethamilselvi Sathiamoorthy, Hemalatha Balasundaram, Oluwole Daniel Makinde, ... Mohamed Altanji, *Alexandria Engineering Journal*In Press, Corrected Proof, Available online 27 June 2022
- [13] Thiyagarajan P, Sathiyamoorthy S, Loganathan K, Makinde OD, Sarris IE. Mass Transfer Effects on the Mucus Fluid with Pulsatile Flow Influence of the Electromagnetic Field. *Inventions*. 2022; 7(3):50. <https://doi.org/10.3390/inventions7030050>
- [14] Thiyagarajan P, Sathiamoorthy S, Santra SS, Ali R, Govindan V, Noeiaghdam S, Nieto JJ. Free and Forced Convective Flow in Pleural Fluid with Effect of Injection between Different Permeable Regions. *Coatings*. 2021; 11(11):1313. <https://doi.org/10.3390/coatings11111313>
- [15] Padmavathi T., Senthamilselvi S., Santra S. S., Govindan V., Altanji M., Noeiaghdam S. Rotational Reaction over Infected Covid-19 on Human Respiratory Tract in the Presence of Soret Effect with Hall Current. *The Bulletin of Irkutsk State University. Series Mathematics*, 2022, vol. 40, pp. 15–33. <https://doi.org/10.26516/1997-7670.2022.40.15>